HHS Public Access

Author manuscript

Adv Mater. Author manuscript; available in PMC 2018 October 01.

Published in final edited form as:

Adv Mater. 2017 October ; 29(40): . doi:10.1002/adma.201703702.

A Eutectic Mixture of Natural Fatty Acids Can Serve as the Gating Material for Near-Infrared-Triggered Drug Release

Dr. Chunlei Zhu,
The Wallace H. Coulter Department of Biomedical Engineering, Georgia Institute of Technology and Emory University, Atlanta, GA 30332, USA

Dr. Da Huo,
The Wallace H. Coulter Department of Biomedical Engineering, Georgia Institute of Technology and Emory University, Atlanta, GA 30332, USA

Qiaoshan Chen,
The Wallace H. Coulter Department of Biomedical Engineering, Georgia Institute of Technology and Emory University, Atlanta, GA 30332, USA

Dr. Jiajia Xue,
The Wallace H. Coulter Department of Biomedical Engineering, Georgia Institute of Technology and Emory University, Atlanta, GA 30332, USA

Dr. Song Shen, and
The Wallace H. Coulter Department of Biomedical Engineering, Georgia Institute of Technology and Emory University, Atlanta, GA 30332, USA

Prof. Younan Xia
The Wallace H. Coulter Department of Biomedical Engineering, Georgia Institute of Technology and Emory University, Atlanta, GA 30332, USA. School of Chemistry and Biochemistry, Georgia Institute of Technology, Atlanta, GA 30332, USA

Abstract

A smart release system responsive to near-infrared (NIR) light has been developed for intracellular drug delivery. We demonstrate the concept by co-encapsulating doxorubicin (DOX, an anticancer drug) and IR780 iodide (IR780, a NIR-absorbing dye) into nanoparticles made of a eutectic mixture of naturally occurring fatty acids. The eutectic mixture has a well-defined melting point at 39 °C, which can be used as a biocompatible phase-change material for NIR-triggered drug release. The resultant nanoparticles exhibit prominent photothermal effect and quick drug release in response to NIR irradiation. Fluorescence microscopy analysis indicates that the DOX trapped in the nanoparticles can be efficiently released into the cytosol under NIR irradiation, resulting in enhanced anticancer activity. This work offers a new platform for designing effective intracellular drug release systems, holding great promise for future cancer therapy.

Correspondence to: Younan Xia.

Supporting Information

Supporting Information is available from the Wiley Online Library or from the author.

Graphical Abstract

A smart system responsive to near-infrared (NIR) light is developed by co-encapsulating a drug and a NIR-absorbing dye into nanoparticles made of a eutectic mixture of naturally occurring fatty acids. Photothermal heating under NIR irradiation facilitates rapid and efficient intracellular drug release, leading to enhancement in anticancer activity.

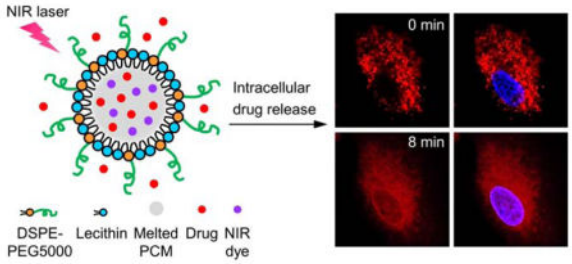

Keywords

phase-change materials; fatty acids; intracellular drug release; drug delivery; cancer therapy

Significant progress has been made in developing smart systems for applications in on-demand drug release.[1] Different from their counterparts for sustained release, the smart systems typically exhibit fast responses to a variety of stimuli, including light,[2] temperature,[3] ultrasound,[4] pH,[5] mechanical stress,[6] and specific biomolecules.[7] Among the various types of stimuli, light is especially attractive because it can be remotely applied with high spatial and temporal resolutions.[8] In view of the deep penetration capability of near-infrared (NIR) light in soft tissues, a number of NIR-responsive systems have been developed,[9] in which most of these systems are built on the conformational changes associated with thermo-responsive polymers to trigger drug release.[10] Despite their popularity, it remains challenging to apply these synthetic polymers to clinic applications, primarily due to their complicated procedures, low degradability, and non-negligible cytotoxicity.[11] Therefore, there is a urgent need to develop a new class of simpler yet more biocompatible thermo-responsive materials for such an application.

In recent years, organic phase-change materials (PCMs) have received considerable interest to serve as a class of thermo-responsive gating materials for drug release.[12] These materials have large latent heat of fusion and exhibit reversible solid-liquid transition over a narrow temperature range. Among those PCMs, natural fatty acids are particularly attractive due to their low cost, chemical stability, and biocompatibility.[13] However, previously reported systems only focused on the use of single-component fatty acids to control drug release. Considering the limited types of natural fatty acids, it is difficult to obtain PCMs with melting points close to the physiological temperature of human bodies (37 °C).[14] In addition, pure saturated fatty acids tend to crystallize upon cooling from a melt; the encapsulated drugs are thus prone to exclusion from the hydrophobic core, generating a drug-rich outer layer and thus undesired burst release.[15] To circumvent these drawbacks, a eutectic mixture of two (or even more) fatty acids, with a melting point lower than that of either of its components, can be used to extend the available melting points and, at the same

time, alter the crystallization behavior of single-component fatty acids to increase the drug loading capacity.[16]

In this work, a eutectic mixture of two fatty acids is used as the gating material to construct NIR-responsive nanoparticles for drug release (Scheme 1). The eutectic mixture, formulated from lauric acid (m. p. = 44 °C) and stearic acid (m. p. = 69 °C) at a weight ratio of 4:1, exhibits a sharp melting point at 39 °C (Figure 1A). It is worth noting that if the fatty acids were not mixed at the eutectic ratio, more than one endothermic peaks would be found in the DSC curve. As naturally occurring fatty acids, both lauric acid and stearic acid are biocompatible and biodegradable.[16,17] Compared to many other fatty acids, they have favorable effects on the increase of “good” blood cholesterol (high-density lipoprotein) and decrease of “bad” blood cholesterol (high-density lipoprotein), respectively, which are preferred in decreasing the atherosclerotic risk.[18] As such, these two fatty acids can be safely used for drug delivery. To trigger melting by NIR light, we encapsulated an appropriate NIR dye in the nanoparticles. Below the eutectic point, the nanoparticles exist in the solid state, preventing the payloads from leaking out through diffusion. Upon NIR irradiation, the nanoparticles will be quickly heated up as a result of the photothermal effect of the encapsulated dye. When the local temperature is increased beyond the eutectic point, the nanoparticles will melt, leading to quick release of payloads.

We fabricated the PCM nanoparticles using a method derived from nanoprecipitation.[19] Briefly, the eutectic mixture of lauric acid and stearic acid was dissolved in methanol and added dropwise into an aqueous solution of phospholipids to promote nanoparticle formation through a self-assembly process. Followed by vigorous vortex, the suspension was cooled down with ice water to rapidly solidify the as-formed nanoparticles. The resultant nanoparticles were then washed with water and purified by ultracentrifugation at temperatures below the eutectic point. We used transmission electron microscopy (TEM) to characterize the nanoparticles. As shown in Figure 1B, the PCM nanoparticles were spherical in shape, together with relatively uniform sizes in the range of 20–70 nm. The distribution of particle size was further analyzed using dynamic light scattering (DLS). The hydrodynamic diameters of the nanoparticles were slightly increased to the range of 50–90 nm (Figure 1C), primarily due to the inclusion of solvation shell.[20] It should be emphasized that we only used naturally-occurring compounds or polymers already approved by the Food and Drug Administration (FDA) to ensure biocompatibility of the resultant nanoparticles.

As a proof of concept, we used doxorubicin (DOX) as a model anticancer drug and IR780 iodide (IR780) as a NIR-absorbing dye.[7a,21] Based on the characteristic absorption spectra shown in Figure 1D, we confirmed the successful loading of both DOX and IR780, with encapsulation efficiency as high as 50.3 ± 3.3% and 59.0 ± 2.2%, respectively. The drug loading contents were further determined to be 2.3 ± 0.1% and 2.8 ± 0.2%, respectively, for DOX and IR780. It is worth noting that after encapsulation, the absorption peak of IR780 was red-shifted by 10 nm from 780 to 790 nm, together with broadening, probably due to the hydrophobic interaction between IR780 and the PCM matrix.[21b,22] The red-shifted, broadened absorption peak makes it easier to overlap with the 808-nm NIR diode laser widely used in chemical and biomedical applications.[21b,23] DLS measurement indicates that the particles were slightly enlarged to 60–110 nm after encapsulation of the payloads

(Figure S1A). In comparison, we also tested single-component fatty acids for the encapsulation of payloads. The nanoparticles made of either lauric acid or stearic acid exhibited significantly decreased encapsulation efficiency due to their high crystallinity upon solidification (Table S1). This finding further highlights the advantage of using a eutectic mixture of fatty acids for improvement in drug loading.

We then evaluated the photothermal properties of the PCM nanoparticles loaded with both DOX and IR780 (denoted DOX/IR780 NPs). As shown in Figure 2A, free IR780 led to moderate photothermal heating as the temperature only rose by six degrees after 5 min of laser irradiation (808 nm, 0.4 W cm^{-2}). In contrast, a more pronounced temperature increase from 22 to 43 °C was observed for the suspension of DOX/IR780 NPs, indicating the enhancement in photothermal heating due to the increased solubility of IR780 in the PCM. We also compared the photothermal effects of free IR780 and DOX/IR780 NPs during repeated laser irradiation (Figure 2B). Free IR780 had very poor photostability so its photoactivity quickly dropped even just after one cycle of laser irradiation. Although there was a drop in photothermal heating, the temperature increase for the DOX/IR780 NPs in the third cycle was still higher than that of free IR780 in the first cycle. Such a difference can be attributed to the fast degradation of free IR780, as confirmed by the disappearance of absorption peak after 4 min of irradiation (Figure S2). To better understand the difference in photothermal behavior, a fluorogenic probe based on 2′,7′-dichlorofluorescin (DCFH) was used to assess the production of reactive oxygen species (ROS).[24] In the presence of ROS, non-fluorescent DCFH will be oxidized and converted to the highly fluorescent 2′,7′-dichlorofluorescein (DCF). During 5 min of laser irradiation, free IR780 led to the production of more ROS, and the fluorescence enhancement ratio was almost twice as strong as that of the DOX/IR780 NPs (Figure 2C). Since free IR780 was directly dissolved in water, it was much easier for the excited IR780 to sensitize the surrounding oxygen molecules, which, in turn, imposed a destructive effect on IR780. For the DOX/IR780 NPs, IR780 was dissolved in the matrix of fatty acids so the production of ROS was greatly inhibited due to the shielding effect of PCM.

To quantify the drug release, the DOX/IR780 NPs were subjected to NIR irradiation while the released amounts were recorded. As the irradiation time was prolonged, the release of DOX was gradually increased (Figure 2D). In comparison, no noticeable drug release was observed for the control group without laser irradiation, indicating that the release of DOX was triggered by the photothermal heating of IR780 and subsequent temperature-induced phase change of PCM. We also performed heating/cooling cycles to further confirm the photothermal-controlled drug release. As shown in Figure S3, DOX release was only observed upon the irradiation of NIR laser. IR780 has a lipophilic structure, whereas the loaded DOX is in the hydrochloride form and thus more hydrophilic. As such, DOX tends to enter the aqueous phase upon PCM melting while IR780 prefers to stay in the hydrophobic PCM. DLS measurement indicates that the PCM nanoparticles did not exhibit significant change in size distribution after 8 min of NIR irradiation (Figure S1B). However, the percentage of particles with diameters ranging from 80–120 nm was relatively increased. We also examined the DOX/IR780 nanoparticles before and after the laser irradiation (Figure S1). The laser irradiation led to some changes to the particle size, which could be attributed to the coalesce of nanoparticles due to the melting of PCM.

We hypothesize that the increase in temperature above the melting point of the PCM will quickly trigger intracellular release of the encapsulated drugs from the melted PCM. To validate this hypothesis, we investigated the intracellular localization of DOX in A549 human non-small cell lung cancer cells. We first examined the intracellular uptake pathway. After co-incubation of the DOX/IR780 NPs with A549 cells for 3 h, we observed a highly co-localized fluorescence of DOX and Lysotracker, suggesting that the DOX/IR780 NPs entered cells *via* an endolysosomal pathway (Figure 3, A–D). We then monitored the intracellular drug release under continuous laser irradiation under fluorescence microscopy. Before laser irradiation, DOX was largely restricted to the endolysosomes, as indicated by the characteristic punctate pattern (Figure 3E). After irradiation with the NIR laser for 4 min, DOX started to move from the acidic compartments to the cytosol, as characterized by the blurred and diffusive fluorescence (Figure 3F). Meanwhile, some DOX was found to accumulate in the periphery of the nucleus. At 8 min post irradiation, the distribution of DOX in the cytosol became more homogenous, with a barely recognized punctate pattern. More importantly, the nuclear shape was clearly outlined by the fluorescence of DOX. Further analysis suggests that the mean fluorescence intensity ratios of the nuclear and cytoplasmic regions were increased by 2.8- and 5.9-fold at 4 and 8 min post irradiation, respectively, indicating that a large amount of DOX escaped from the endolysosomes and intercalated into the nuclear DNA (Figure S4). As controls, both DOX-loaded nanoparticles (denoted DOX NPs) and free DOX were tested under the same conditions. As shown in Figure S5, neither of them exhibited noticeable change in DOX distribution, confirming the effectiveness of the NIR-triggered drug release. It should be pointed out that since the internalized PCM nanoparticles were primarily localized in the endolysosomes, it would be useless if the released drugs did not escape from these acidic compartments and diffuse into the cytosol. As discussed above, NIR irradiation of IR780 can sensitize the production of ROS, which gives rise to the destabilization of the endolysosomal membranes to facilitate cytosolic diffusion of the drug.[25] These results demonstrate that NIR irradiation not only initiates DOX release from the PCM nanoparticles but also facilitates the endolysosomal escape of DOX.

We further evaluated the NIR-triggered anticancer activity of the DOX/IR780 NPs using cell viability assay. As shown in Figure 4, the DOX/IR780 NPs exhibited dose-dependent dark cytotoxicity against A549 cells due to the release of a small amount of DOX and IR780 in the acidic endolysosomes. After NIR irradiation at 0.2 W cm^{-2} for 8 min, the DOX/IR780 NPs showed significantly increased anticancer activity. When the concentration of IR780 in the DOX/IR780 NPs reached 2.00 μg mL^{-1}, the cells only maintained *ca.* 6% cell viability, which is 10 times as low as that of the cells without laser irradiation. In contrast, laser irradiation alone did not cause any change in viability for the A549 cells. In view of the cytotoxicity of DOX, as well as the photothermal and photodynamic effects of IR780, we also performed control experiments to analyze the contributions from DOX NPs and IR780-loaded nanoparticles (denoted as IR780 NPs) to the cytotoxicity at the highest concentration. No obvious dark cytotoxicity was observed for DOX NPs and laser irradiation did not induce noticeable change in cell viability either, probably due to the inefficient drug release from the solid PCM. Such a result further demonstrates that only the NIR-triggered phase-change can effectively lead to the cytosolic drug delivery. IR780 NPs, however, also

exhibited marked cytotoxicity upon laser irradiation, leading to *ca.* 67% cell death relative to the dark cytotoxicity of IR780 NPs. As for the DOX/IR780 NPs, NIR irradiation induced *ca.* 90% cell death. The additional cytotoxicity should be attributed to the NIR-triggered DOX release, and the observed cytotoxicity of the DOX/IR780 NPs is a combination of the anticancer effect of the released DOX and the photothermal effect of IR780. In this proof-of-concept study, we used IR780 as a NIR dye to demonstrate the photothermal-controlled drug release. In spite of the gating effect of the PCM matrix, the harsh conditions in the acid endolysosomes inevitably resulted in some minor release of IR780, which had a non-negligible impact on cell viability. This issue can be readily addressed by switching to other more biocompatible NIR dyes.[26]

In summary, we have demonstrated the fabrication of fatty acid-based PCM nanoparticles for NIR-triggered drug release. To ensure biocompatibility, the components used for nanoparticle fabrication are either from natural sources or from FDA-approved biocompatible polymers. In a proof of concept experiment, the anticancer drug DOX and NIR dye IR780 were also loaded in the PCM matrix. The use of a mixture of fatty acids reduced the crystallinity of the matrix upon solidification, greatly increasing the drug loading efficiency. Further studies indicate that DOX/IR780 NPs exhibited prominent photothermal effect as well as quick drug release in response to NIR irradiation. Fluorescence microscopy analysis suggests that these nanoparticles entered cells *via* the endolysosomal pathway. Upon irradiation with a NIR laser, we observed an efficient and rapid intracellular release of DOX from the melted PCM, leading to the enhancement in anticancer activity. In the future study, functionalization of the PCM nanoparticles with tumor-targeting ligands will be explored to achieve targeted drug delivery.

Supplementary Material

Refer to Web version on PubMed Central for supplementary material.

Acknowledgments

This work was supported in part by a grant from the National Institutes of Health (R01 EB020050) and startup funds from the Georgia Institute of Technology.

References

1. a) Liu D, Yang F, Xiong F, Gu N. Theranostics. 2016; 6:1306. [PubMed: 27375781] b) Blum AP, Kammeyer JK, Rush AM, Callmann CE, Hahn ME, Gianneschi NC. J Am Chem Soc. 2015; 137:2140. [PubMed: 25474531] c) Mura S, Nicolas J, Couvreur P. Nat Mater. 2013; 12:991. [PubMed: 24150417]
2. a) You J, Zhang G, Li C. ACS Nano. 2010; 4:1033. [PubMed: 20121065] b) Kohman RE, Cha SS, Man HY, Han X. Nano Lett. 2016; 16:2781. [PubMed: 26935839] c) Meng Z, Wei F, Wang R, Xia M, Chen Z, Wang H, Zhu M. Adv Mater. 2016; 28:245. [PubMed: 26551334]
3. a) Ma C, Shi Y, Pena DA, Peng L, Yu G. Angew Chem Int Ed. 2015; 54:7376.b) Al-Ahmady ZS, Al-Jamal WT, Bossche JV, Bui TT, Drake AF, Mason AJ, Kostarelos K. ACS Nano. 2012; 6:9335. [PubMed: 22857653]
4. a) Zhang K, Xu H, Jia X, Chen Y, Ma M, Sun L, Chen H. ACS Nano. 2016; 10:10816. [PubMed: 28024356] b) Epstein-Barash H, Orbey G, Polat BE, Ewoldt RH, Feshitan J, Langer R, Borden MA, Kohane DS. Biomaterials. 2010; 31:5208. [PubMed: 20347484] c) Tang H, Zheng Y, Chen Y. Adv Mater. 2017; 29:1604105.

5. a) Wang Y, Song S, Liu J, Liu D, Zhang H. Angew Chem Int Ed. 2015; 54:536.b) Muharnmad F, Guo M, Qi W, Sun F, Wang A, Guo Y, Zhu G. J Am Chem Soc. 2011; 133:8778. [PubMed: 21574653]
6. a) Hyun DC, Moon GD, Park CJ, Kim BS, Xia Y, Jeong U. Angew Chem Int Ed. 2011; 50:724.b) Zhang Y, Yu J, Bomba HN, Zhu Y, Gu Z. Chem Rev. 2016; 116:12536. [PubMed: 27680291]
7. a) Mo R, Jiang T, DiSanto R, Tai W, Gu Z. Nat Commun. 2014; 5:3364. [PubMed: 24618921] b) Guo DS, Wang K, Wang YX, Liu Y. J Am Chem Soc. 2012; 134:10244. [PubMed: 22686862]
8. a) Rai P, Mallidi S, Zheng X, Rahmanzadeh R, Mir Y, Elrington S, Khurshid A, Hasan T. Adv Drug Deliv Rev. 2010; 62:1094. [PubMed: 20858520] b) Fan NC, Cheng FY, Ho JA, Yeh CS. Angew Chem Int Ed. 2012; 51:8806.
9. Rwei AY, Wang W, Kohane DS. Nano Today. 2015; 10:451. [PubMed: 26644797]
10. a) Yavuz MS, Cheng Y, Chen J, Cobley CM, Zhang Q, Rycenga M, Xie J, Kim C, Song KH, Schwartz AG, Wang LV, Xia Y. Nat Mater. 2009; 8:935. [PubMed: 19881498] b) Zhang Z, Wang J, Nie X, Wen T, Ji Y, Wu X, Zhao Y, Chen C. J Am Chem Soc. 2014; 136:7317. [PubMed: 24773323]
11. a) Nykänen A, Nuopponen M, Laukkanen A, Hirvonen SP, Rytelä M, Turunen O, Tenhu H, Mezzenga R, Ikkala O, Ruokolainen J. Macromolecules. 2007; 40:5827.b) Shao P, Wang B, Wang Y, Li J, Zhang Y. J Nanomater. 2011; 2011:389640.c) Vihola H, Laukkanen A, Valtola L, Tenhu H, Hirvonen J. Biomaterials. 2005; 26:3055. [PubMed: 15603800]
12. a) Hyun DC, Levinson NS, Jeong U, Xia Y. Angew Chem Int Ed. 2014; 53:3780.b) Hyun DC, Lu P, Choi SI, Jeong U, Xia Y. Angew Chem Int Ed. 2013; 52:10468.c) Choi SW, Zhang Y, Xia Y. Angew Chem Int Ed. 2010; 49:7904.d) Moon GD, Choi SW, Cai X, Li W, Cho EC, Jeong U, Wang LV, Xia Y. J Am Chem Soc. 2011; 133:4762. [PubMed: 21401092]
13. Yuan Y, Zhang N, Tao W, Cao X, He Y. Renew Sust Energ Rev. 2014; 29:482.
14. a) Kumar S, Randhawa JK. RSC Adv. 2015; 5:68743.b) Xie S, Zhu L, Dong Z, Wang Y, Wang X, Zhou WZ. Int J Nanomed. 2011; 6:547.
15. a) Phan S, Salentinig S, Gilbert E, Darwish TA, Hawley A, Nixon-Luke R, Bryant G, Boyd BJ. J Colloid Interf Sci. 2015; 449:160.b) Müller RH, Mäder K, Gohla S. Eur J Pharm Biopharm. 2000; 50:161. [PubMed: 10840199]
16. a) Zhao P, Yue Q, He H, Gao B, Wang Y, Li Q. Appl Energ. 2014; 115:483.b) Zhu C, Pradhan P, Huo D, Xue J, Shen S, Roy K, Xia Y. Angew Chem Int Ed. 2017; doi: 10.1002/anie.201704674
17. Nelson, DL., Cox, MM. Lehninger Principles of Biochemistry. 5. W. H. Freeman and Company; New York: 2008.
18. a) Mensink RP, Zock PL, Kester ADM, Katan MB. Am J Clin Nutr. 2003; 77:1146. [PubMed: 12716665] b) Hunter JE, Zhang J, Kris-Etherton PM. Am J Clin Nutr. 2010; 91:46. [PubMed: 19939984]
19. a) Zhang L, Chan JM, Gu FX, Rhee JW, Wang AZ, Radovic-Moreno AF, Alexis F, Langer R, Farokhzad OC. ACS Nano. 2008; 2:1696. [PubMed: 19206374] b) Chan JM, Zhang L, Yuet KP, Liao G, Rhee JW, Langer R, Farokhzad OC. Biomaterials. 2009; 30:1627. [PubMed: 19111339]
20. Kumar A, Pandey AK, Singh SS, Shanker R, Dhawan A. Cytom Part A. 2011; 79a:707.
21. a) Yuan A, Qiu X, Tang X, Liu W, Wu J, Hu Y. Biomaterials. 2015; 51:184. [PubMed: 25771009] b) Wang K, Zhang Y, Wang J, Yuan A, Sun M, Wu J, Hu Y. Sci Rep. 2016; 6:27421. [PubMed: 27263444]
22. Yan L, Wang H, Zhang A, Zhao C, Chen Y, Li X. J Mater Chem B. 2016; 4:5560. [PubMed: 28944057]
23. Liu B, Li C, Yang P, Hou Z, Lin J. Adv Mater. 2017; 29:1605434.
24. a) Zhu C, Yang Q, Liu L, Lv F, Li S, Yang G, Wang S. Adv Mater. 2011; 23:4805. [PubMed: 21935997] b) Cohn CA, Simon SR, Schoonen MAA. Part Fibre Toxicol. 2008; 5:2. [PubMed: 18307787]
25. Appelqvist H, Wäster P, Kågedal K, Öllinger K. J Mol Cell Biol. 2013; 5:214. [PubMed: 23918283]
26. Hong G, Lantaris A, Dai H. Nat Biomed Eng. 2017; 1:0010.

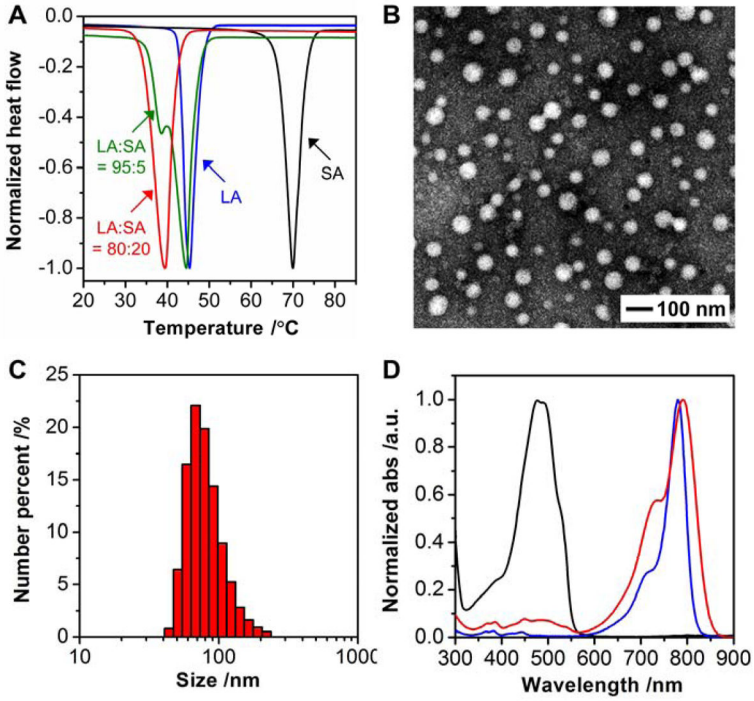

Figure 1.

Characterization of the PCM and its nanoparticles. A) DSC curves of lauric acid (LA) and stearic acid (SA) at different weight ratios. Note that a eutectic mixture was formed at a weight ratio of 80:20 between LA and SA. B) A typical TEM image of the PCM nanoparticles. C) Particle size distribution measured by DLS. D) UV/vis absorption spectra of free DOX (black), free IR780 (blue), and DOX/IR780 NPs (red).

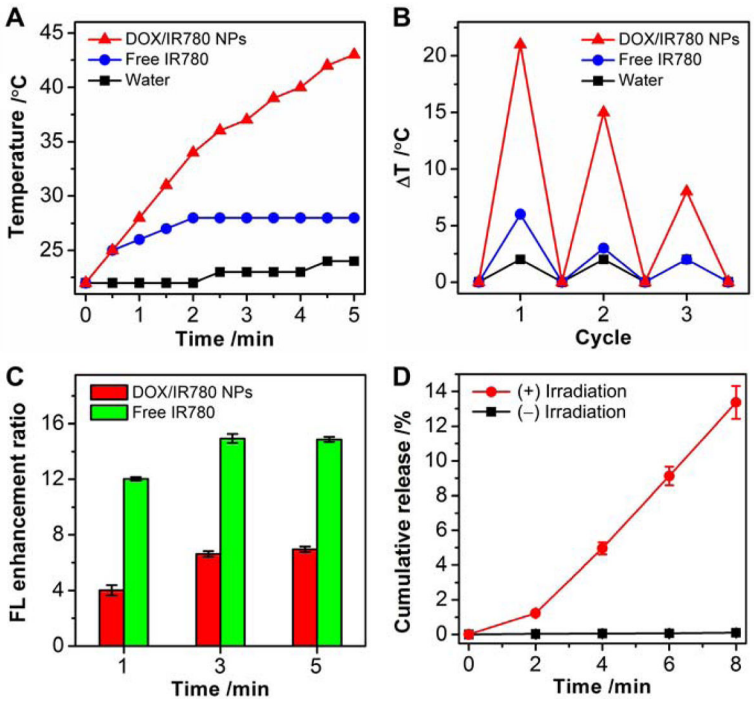

Figure 2.

Photothermal effect of the DOX/IR780 NPs. A) Changes in temperature for a saturated solution of free IR780 and a suspension of the DOX/IR780 NPs upon irradiation by the 808-nm NIR laser at a power density of 0.4 W cm^{-2}. B) Comparison of the photothermal heating behaviors for the free IR780 and DOX/IR780 NPs after repeated cycles of laser irradiation. C) Fluorescence enhancement ratio of DCFH activated by free IR780 and the DOX/IR780 NPs upon laser irradiation at a power density of 0.4 W cm^{-2}. D) Cumulative DOX release from the DOX/IR780 NPs upon laser irradiation at a power density of 0.4 W cm^{-2}.

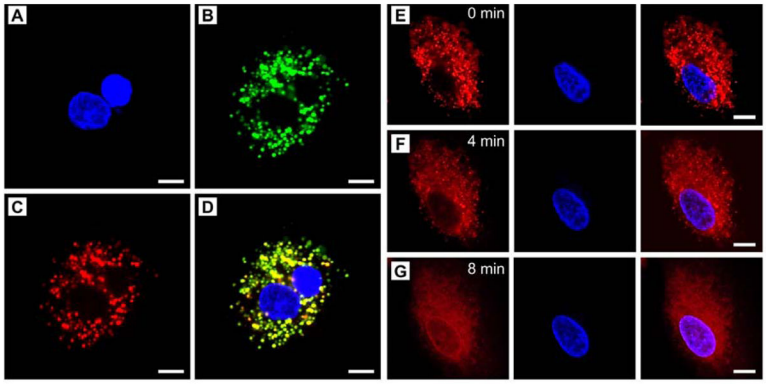

Figure 3.

Cellular uptake of the DOX/IR780 NPs and demonstration of NIR-triggered drug release. A–D) Fluorescence micrographs showing the locations of the DOX/IR780 NPs in A549 cells after incubation for 3 h. A) Hoechst 33342 (blue), B) Lysotracker (green), C) DOX (red), and D) merged image. E–G) Time-course DOX release in response to the 808-nm NIR laser at a power density of 0.2 W cm^{-2}. Scale bars: 10 μm.

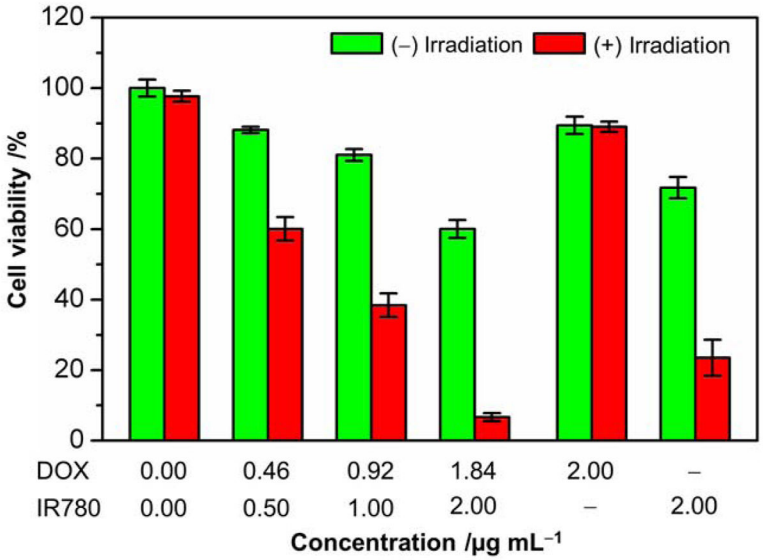

Figure 4.

Cell viability of A549 cells incubated with the DOX/IR780 NPs at different particle concentrations with or without laser irradiation at a power density of 0.2 W cm^{-2} for 8 min.

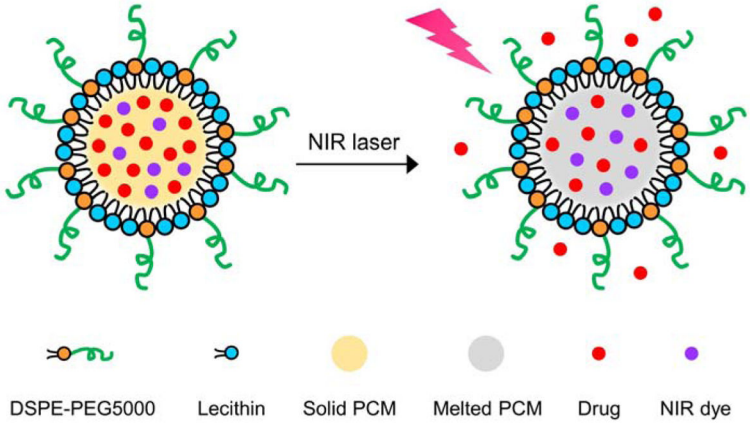

Scheme 1.

Schematic illustration showing the NIR-triggered release of drug molecules from a PCM nanoparticle made of a eutectic mixture of two fatty acids.